Tilting at Neutron Windmills: Neutron-powered micromotor design and theoretical analysis

Whyte A[1]
aw@paramita-electronics.org

ABSTRACT

The Crookes radiometer has existed for over 100 years, with much initial scientific interest. In recent years research has been boosted by applications such as in nanotechnology MEMs devices. It is proposed to investigate a neutron-powered micromotor, based on the same principle. The device converts potential and kinetic energy in neutrons into macroscopic motion by the means of the convection of gas molecules induced by an asymmetric neutron heating. The proposed system has immediate application in neutron detection at high flux, but could be developed to generate useful amounts of power at scales from nanotechnology to bench top systems. Simulated results show that asymmetric heating of the order required can be achieved in devices that are simple to build in the laboratory.

KEYWORDS: MEMs, neutron actuation, neutron heating, energy harvesting, neutron energy, micromotor, knudsen pump, knudsen compressor, neutron mill, crookes radiometer, nanotechnology

1. INTRODUCTION

A Crookes radiometer converts light into kinetic motion and was the first light-powered actuator to be discovered. Its function was discussed by hundreds of scientists, notably Maxwell [1], and Reynolds [2] * before being later more fully explained by Einstein [4] (translation found in [5]), whereupon interest waned. The process is not covered by the Navier-Stokes equations and it has tended to be ignored in thermodynamics literature. A good review of modern theory is found in Martin [6].

The Crookes radiometer, in fact works by converting radiated energy to heat and the heat differential causes gas particles to diffuse selectively across the thermal gradient creating a macro pressure effect. The premise of this paper is that the heat energy released when a neutron is absorbed will have the same effect in the correct conditions.

In this theoretical study, two geometries for possible *neutron micromotor* designs are considered. Firstly a design based on the work of Han *et al.* [7], which uses the geometry of the vanes to encourage light (and in this case neutrons) preferentially onto one side of the vanes is considered. Secondly, a more standard design, using materials that differentially absorb neutrons is considered.

The device is proposed as a sensor that works by measuring the amount of rotation in the device. However the concept of a neutron micromotor is interesting because it is a novel method of generating a macroscopic kinetic movement from energy held in thermal or epithermal neutrons. The authors have not found references in the literature to this kind of direct neutron powered actuation. Although neutrons don't occur abundantly at the earth's surface, in space, and the earth's upper atmosphere, the neutron flux is of an order that could activate a carefully designed device [8]. Neutron flux must be monitored in waste storage and processing plants to ensure that critical mass is not achieved accidentally. It is also important to measure thermal neutron flux in the core of PWR and AGR reactors, potentially an entirely mechanical neutron detector could ensure that measurements continue even when electricity is unavailable.

1.1. Neutron Detectors

Commercially available neutron detectors are categorised as either fast neutron detectors or slow neutron detectors [9]. Although this system may function with fast and slow neutrons, due to the energy dependence of

*For a comprehensive record of the development of scientific theory, see [3]

cross sections, thermal neutrons are considered at this time. Alternative slow neutron detectors include gas proportional detectors, scintillation detectors, semiconductor neutron detectors and Fission chambers.

Proportional gas detectors require either ^3He, which has a restricted global supply, or $^{10}BF_3$ which corrodes stainless steel when mixed with water and is extremely toxic if released from the detector [10].

At high neutron fluxes, pulse counting detectors, such as gas detectors, scintillation and semiconductor devices, suffer from *pulse pile-up*, where multiple pulses amalgamate so electronic counting devices don't separate counts. The proposed design is expected to generate a proportional result even at high fluxes. Fission chambers use a fissile material to detect neutron flux. A disadvantage of these devices is that they can be difficult to source and transport due to restrictions on the fissile content.

The device can be manufactured extremely cheaply, with an estimated manufacturing cost in the $\approx$ 50 USD. This compares favourably with commercial devices which have a cost in the range of hundreds to over ten thousand (depending on the materials and application) [citation needed]. For these reasons there is interest in finding a alternative way to detect thermal neutrons.

1.2. Geometries Considered

Since light can be used to create a heat differential on the vanes of a small 'turbine' shaped micromotor, it was conjectured that the same geometry, designed from a suitable neutron absorber, will also cause a force to be generated. The amount of scattering caused by rarefied gas can be expected to be negligible so most neutrons will travel in straight lines allowing the geometric design used by Han *et al.* [7] to operate. This was the design philosophy of the first geometry investigated *(see Fig. 4)*.

The design aim of the second geometry is to use a neutron absorbing material to capture neutrons, while another material that is less absorbent forms the opposite side of the vanes to produce a temperature differential and subsequent gas convection *(see Fig. 6)*

1.3. Material Choices

Firstly, absorbent materials were considered. The most absorbent, naturally occurring elements are boron, cadmium promethium, samarium, europium and gadolinium. Boron was selected as a potential material, due to its low toxicity, stability, workable compounds and low cost. Gadolinium is also used in PWR reactors and may prove interesting due to the elastic collision of faster than thermal neutrons providing energy without being used up, potentially extending the life of devices.

Crystalline boron is used as a filament material for strength in glass fibre for high performance applications. Controlled geometries can be manufactured using chemical vapour deposition [11]. Since boron is a relatively light element enrichment of the ^{10}B isotope is possible more easily than heavier elements, this opportunity is not investigated in this study.

Boron nitride is a machinable ceramic material that can be purchased online from a number of sources (*e.g. http://www.precision-ceramics.co.uk*) it is available commercially up to extremely high purity grades (AX05 grade has a purity of BN available at 99.7%+ [12]). It is also available as an aerosol spray coating, which is used for covering metals to protect them at high temperatures. This has the advantage that a very thin layer of material can be deposited onto a surface. However the purity grade has not been established.

The energy evolved from the capture of neutrons in boron nitride is described by the following chemical interactions by Deng [13].

Boron neutron capture:

$$^{10}B+^1_0n(0.025eV) \rightarrow^{11} B\begin{cases} ^4He_2 +^7 Li + 2.79MeV(6\%) \\ ^4He_2 +^7 Li + 2.31MeV(94\%) \end{cases}$$

$$^7Li + \gamma + 0.48MeV \qquad (1)$$

Nitrogen neutron capture:

$$^{14}_7N +^1_0 n \rightarrow^{14}_6 C +^1_1 H + 0.66MeV \qquad (2)$$

The released energy is deposited locally except for 0.48 MeV photon energy [13] [14]. Although the amount of photon energy is moderate, it is smaller than the thermal energy and it is expected that the majority of γ photons

will exit the system without interaction. The photon energy has been subtracted in this analysis.

For this project pyrolytic graphite is expected to be used as the support material in geometry 2 due to its low neutron cross section and advantageous heat conduction properties.

Pyrolytic graphite of a suitable thickness is available for the electronics industry (*e.g.* Panasonic EYGS121805) This can be treated with a surface coat of BN aerosol spray to create a suitable vane structure (*e.g.* Saint Gobain 'Combat 'coatings) with dimensions approximately at the level described in geometry II (Fig.6)



Figure 1: Boron nitride with a high purity can be machined into complex geometries (*image: https://precision-ceramics.com/materials/boron-nitride/*)

1.4. Geometric Requirements

According to Einstein [5]([4]) the force on the vanes is maximal when the *Mean Free Path (MFP)*, of the gas particles approaches the thickness of the vanes. This paper uses Einstein's formula [5] for force on vanes with the correction by Martin [6] which applies at optimal pressure.

$$F_{Einsten} = p4L\Lambda\frac{\Delta T}{T} \tag{3}$$

F	N	force on vane
p	$pascal$	gas pressure
L	m	length of vane (assumed to be square)
Λ	m	Mean Free Path
T	K	Temperature

For *MFP = Vane thickness* to be achieved, a low pressure is required to increase the *MFP* to thickness that the vanes can be built. This was confirmed by Han *et al.* [15], who use *Direct Method Monte Carlo (DMMC)* to show that 400 mTorr is optimal for vanes that are about 0.1mm thick. This vacuum pressure is around the upper edge of what can be achieved with a standard, laboratory, positive displacement vacuum pump.

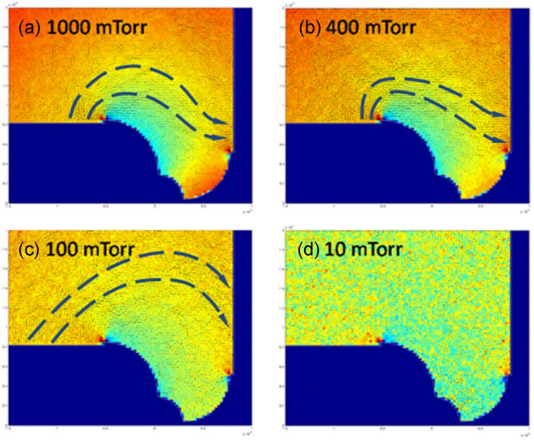


Figure 2: DMMC simulation of pressure at the vane surfaces (image source: [7])

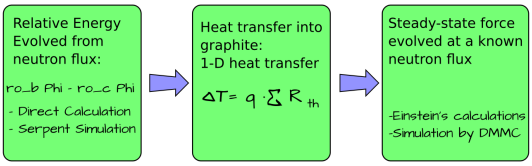


Figure 3: A flow diagram to show the calculation flow)

For initial calculations, a three step plan was proposed as shown in Fig. 3.

1) Initially, the SERPENT [16] *Monte Carlo, (MC)* code was used to estimate the absorption rate of neutrons in the front and back of the vane.

2) From the relative interaction rate, the thermal energy generated is estimated. This is converted into the steady state ΔT, this can be calculated using Fourier's Law for one dimension [17] (simplification: all heat energy lost into rarefied gas on cooler side of vane).

3) Calculation of the evolved force based on ΔT using equation (3) [4], [7].

However, the results of the thermal energy generated was estimated and compared to similar calculations for an existing Crookes radiometer (*see APPENDIX A*). this mean that steps 3 was redundant, though equation 3 is relevant for proposed optimisation of the design.

1.5. Neutron Sources

In APPENDIX A it is estimated that a fluence of 6.7×10^4 thermal neutrons captured on a vane will equal the motion from black body radiation caused by a hand onto a square $1cm^2$ vane. Although this represents an upper threshold for sensitivity than current state of the art neutron detectors, it should be noted that calculations are based on a square vane. Einstein's equation 3 is proportional to the perimeter, so vanes that are made of a grid or comb shape will have a significantly higher response.

An $^{241}Am-^{9}Be$ source is nominally of 1 Ci is used in Cambridge Engineering demonstrations. At the source, this generates approximately 2.4×10^6 (fast) neutrons.

The VR-1 sparrow research reactor achieves a peak thermal neutron flux of 2×10^9 nv. It is available for collaborative work if they are credited in published research and commercial research on a case by case basis.

2. GEOMETRY I

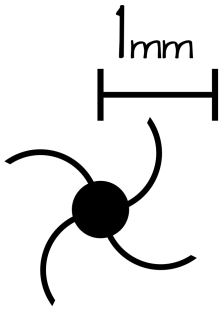


Figure 4: Device designed from a single material

The first geometry investigated in this study (Fig. 4), resembles the geometry developed by Han *et al.* [15]. Curved blades expose the convex side to external incoming neutrons more effectively than the concave side. Based on the size of the device, it is shown in APPENDIX B that the MFP of neutrons in boron nitride was much larger than the vane thickness. In order to maximise the gradient across the vanes this experiment uses α-rhombohedral crystalline boron as the material for the device. Enrichment of the ^{10}B content would further improve performance but was not simulated at this time.

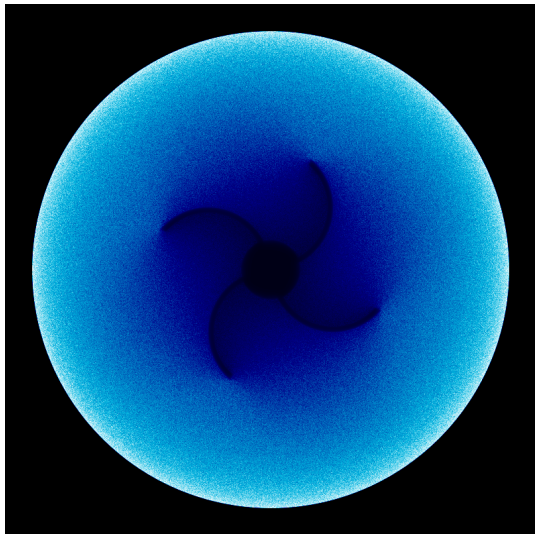


Figure 5: Geometry 1 flux map shows higher flux at the leading edge of the vanes.

2.1. Serpent Simulation:Geometry I

In simulation, the device is placed in a rarefied nitrogen atmosphere of 4mm radius. The simulation has 'black' boundary conditions at 10mm. A cylindrical source of thermal neutrons (0.025eV) made of void material surrounds the device assembly with a thickness of 0.5mm. Absorption detectors are placed in the convex side and the concave side of a vane to record the number of absorptions and surface detectors at the outside of the rarefied gas tally the rate neutrons enter the experiment allowing an estimate of the fluence.

Flux is generated isotropically in a cylinder surrounding the device assembly shown in Fig. 5. A cylindrical source is considered a good approximation of

a directional source averaged over the rotation of the device. The inner gas cylinder is rarefied nitrogen at $400mTorr$. The device is as shown in Fig. 4. To avoid neutron direction becoming biased, 'black' boundary conditions were used for the outside of the simulation, neutrons that travel outside the simulation are erased. This means that only flux that enters the rarefied gas is considered (though it may or may not interact while inside the cylinder).

The flux density map evolved by the simulation is shown in Fig. 5, it can be seen from the image that the neutron flux immediately adjacent to the concave side of the vanes is depressed compared to the convex side of the vanes. The simulation shows that the fraction of generated neutrons that enter the experiment is 0.31308 and that the convex side of the blade receives 58.90 % more neutron absorptions than the concave side.

Table 1: Geometry 1 results in serpent

Inward fluence captured	54.291	%
Capture in boron	100	%
Extra capture in convex side	17.457	%
mean fluence needed to equal hand in a $1cm^2$ sensor	7.1653×10^5	nv

From this simulation it is possible to work backwards to establish the neutron fluence required to generate the number of neutrons estimated in APPENDIX A. The calculations in table tab:geom1calcs compares the maximum energy from a weak light source known to turn a consumer Crookes Radiometer with the average energy imparted by a neutron fluence. So, although it not a like for like comparison, it does give an estimate for the flux required for a basic device to be tested.

Table 2: Geometry 1 Summary

Advantages	Disadvantages
Single material, advantageous for vapour deposition manufacture	Lower absorption difference between sides of vanes
	Requires vapour deposition manufacture in boron

3. GEOMETRY II

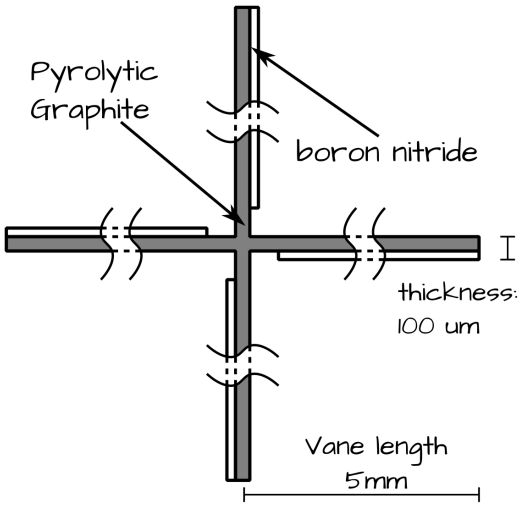


Figure 6: The dual material device design

The second geometry, shown in Fig. 6, considered benefits from being relatively simple to manufacture, using off-the-shelf components such as pyrolytic graphite sheet and boron nitride aerosol sprays.

3.1. Serpent Simulation:

The second geometry flux map shown in Fig. 7 shows much more absorption in the boron nitride than the graphite. In fact the simulation results show that 99.998% of all capture is occurring in the boron nitride layer. Since the neutrons are thermal there is no net energy transferred by elastic collisions so only capture is considered in these results.

As before, the source is isotropic and surrounds the device to simulate the net absorption of rotating vanes from a directional source.

Flux is generated isotropically in a cylinder surrounding the device assembly shown in Fig. 6. The inner gas cylinder is rarefied nitrogen at $400mTorr$.

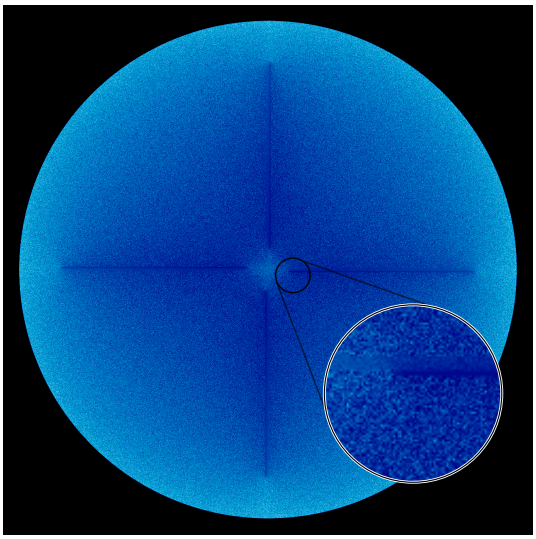


Figure 7: The dual material device flux map (inset shows graphite vane with boron coating on bottom side)

4. DISCUSSION AND LIMITATIONS OF THE THEORETICAL APPROACH

This study shows that the design would likely work. It also generates some calculations that imply that the fluence required to cause rotation in geometry II is not far from those available in the lab. Improvements, like increasing the perimeter of the device have not been considered, though it is known to be linearly dependent, so increasing the response many times for a given size of detector could be expected.

Table 3: Geometry 2 results on serpent

Inward fluence captured	18.536	%
Capture in BN	99.9998	%
mean fluence needed to equal hand in a $1cm^2$ sensor	1.2587×10^4	nv

Table 4: Geometry 2 Summary

Advantages	**Disadvantages**
Simple to build for experiments	Harder to miniaturize
More efficient operation	

5. CONCLUSIONS

Two potential geometries have been investigated for a novel method of neutron detection. If successful then this method of neutron detection could have interesting properties that current neutron detectors lack; it may avoid reliance on ^3He and can be manufactured with compounds that are largely non-toxic, it would not be affected by saturation due to pulse pile up effects and could be extremely cheap to build.

This study provides a case for further investigation of this design idea. Although neutrons deliver many thousands of times the energy of photons, the scarcity of neutrons compared to photons makes effecting mechanical work from them difficult. The calculations in this paper imply that it will be possible to observe the intended phenomena, harvesting energy from the absorption of a neutron by boron or boron-nitride. Despite the low expected thermal efficiency of the system, it may be the first description of a micro-generation technique using neutron reactions as well as a novel sensor design.

APPENDIX A. Calculations of light heating

Although neutrons impart approximately 10^6 times more energy on absorption than a photon, photons often outnumber neutrons by 10^{10} in laboratory situations. The following example calculations show the amount of energy that can be expected from different light systems and the neutron flux required to equal the light energy.

Energy of a photon:

$$E = hf = hc/\lambda \tag{4}$$

So a photon of $500nm$ wavelength has:

$$E = (6.626 \times 10^{-34}\,\mathrm{J}s)(3 \times 10^8\,\mathrm{m}/s)/(700 \times 10^{-9}\,\mathrm{m})$$
$$= 3.9756 \times 10^{-19}\,\mathrm{J} = 2.48eV \tag{5}$$

A lamp creates 15W of photons, so the intensity at 1m is:

$$I = P_{lamp}/(4\pi R^2)I = (15/(4\pi) \quad (6)$$

A vane of a Crookes Radiometer is around 15mm x 15mm. So:

$$A = (0.015m)(0.015m) = 0.000225m^2 \quad (7)$$

So the Power of photons onto the vane at 1m is:

$$P_{vane} = IA \quad (8)$$

$$P_{vane} = (15/(4 * \pi * 1^2)) * (0.000225)$$
$$= 268.5\mu Watts(1.675\,85 \times 10^9\,MeV)$$

Or

$$= 0.0002685/3.9756 \times 10^{-19}\,Joules$$
$$= 6.7556 \times 10^{14}\,photons$$

A Crookes radiometer used in experiments can be activated by the heat from a hand held close enough to the glass to warm it up. Assuming that there is a perfect transfer from a hand at 15cm from the vane and the hand is at $37^oC(310.15K)$

So total radiated energy from a palm that is 10cm $\times$ 10cm would be:

$$u(T) = \frac{4\pi}{c}\int_0^\infty B_\nu(T)d\nu * \frac{0.1^2}{4\pi 0.15^2} \quad (9)$$

and by Planck's Law:

$$B_\nu(T) = \frac{2h\nu^2}{c^2}\frac{1}{e^{h\nu/kT} - 1} \quad (10)$$

Substitute $K_1 = 2h/c^2$ & $K_2 = h/k_BT$ then:

$$u(T) = \frac{4\pi}{c}\int_0^\infty \frac{K_1\nu^3}{e^{K_2\nu} - 1}d\nu * 0.0044 \quad (11)$$

So:

$$u(T) = 4.1917 \times 10^{-8} * 167.0122 * 0.0044 \quad (12)$$

$$= 3.0803 \times 10^{-8}\,joules \quad (13)$$

Equivalent to 194197.88 MeV or around 104474.87 neutron absorptions per second in the hot side of the vane. It is reasonable to assume that the silvered side reflects $60 - 70\%$ of photons, while the dark side reflects 5%

This would change the energy differential on the black vane to:

$$= (194197.88 * 0.95) - (194197.88 * 0.3)$$
$$= 126228.622MeV$$
$$= 67908.663 \text{ neutrons (mean } 1.88MeV)$$

Assumptions: considers only the light landing on a perpendicular vanes. Mixture of point source and area used.

APPENDIX B. Calculation of mean free path of a neutron in Boron and Boron Nitride

Density:

$$\begin{aligned} M_B &= 10.8 \\ M_N &= 14 \\ M_{Mixture} &= 10.8 + 14 \text{ g/mol} \\ \rho &= 2.25\ g/cm^3 \\ N_{BN} &= \rho.N_a/M_{Mixture} \\ &= (2.25g/cm^3) \times (6.02 \times 10^{23}\,nuclei/mol) \\ &\quad \times (10.8 + 14g/mol) \\ &= 5.461\,693\,5 \text{ molecules of } BN/cm^3 \end{aligned}$$

Microscopic cross-section:

$$\begin{aligned} N_{B10} &= 5.461\,693\,5 \times 10^{22} \times 0.199 = 1.086\,877\,0 \times 10^{22} \\ N_{B11} &= 5.461\,693\,5 \times 10^{22} \times 0.801 = 4.374\,816\,5 \times 10^{22} \\ N_N &= 5.461\,693\,5 \times 10^{22} \end{aligned}$$

$$\begin{aligned} \sigma^{10B} &= 3843 \text{ b of which } \rho^{10B}_{n,alpha} = 3840b \\ \sigma^{11B} &= 5.07 \text{ b} \\ \sigma^{14N} &= 11.01 \text{ b} \end{aligned}$$

Macroscopic cross-section:

$$\begin{aligned} \Sigma_t^{BN} &= 3842 \times 10^{-24} \times 1.086\,877\,0 \times 10^{22} + \\ &\quad 5.07 \times 10^{-24} \times 4.374\,816\,5 \times 10^{22} + \\ &\quad 11.01 \times 10^{-24} \times 5.461\,693\,5 \times 10^{22} \\ &= 41.75 + 0.26 + 0.60 \\ &= 42.6203cm^{-1} \end{aligned}$$

So the *MFP*:

$$\Lambda = 1/\Sigma_t^{BN} \approx 0.234mm \quad (14)$$

This is much larger than the thickness of the vanes at acceptable pressures, this means that geometry 1 (*see section 2*) will likely have low efficiency when made from

boron nitride An enriched ^{10}B device would have much better efficiency, though this paper considered only natural boron.

$$
\begin{aligned}
N_{B_{10}} &= \rho.N_a/M_{Mixture} \\
&= (2.08g/cm^3) \times (6.02 \times 10^{23}\,\mathrm{n}uclei/mol) \\
&= 1.252\,16 \times 10^{25} \\
&- \\
\Sigma_t^{B10} &= 3842.0 \times 10^{-24} \times 1.252\,16 \times 10^{25}\ . \\
&= 48107.9872
\end{aligned}
$$

$\approx 2.08g/cm3$ Density $\approx 2.08g/cm3$

so *MFP*:

$$\Lambda = 1/\Sigma_t^{B10} \approx 20.7865\mu m \tag{15}$$

REFERENCES

[1] J. C. Maxwell. "VII. On stresses in rarified gases arising from inequalities of temperature." *Philosophical Transactions of the royal society of London*, **volume 170**, pp. 231–256 (1879).

[2] O. Reynolds et al. "XVIII. On certain dimensional properties of matter in the gaseous state." *Philosophical Transactions of the Royal Society of London*, **volume 170**, pp. 727–845 (1879).

[3] S. G. Brush. *The kind of motion we call heat: A history of the kinetic theory of gases in the 19th century (Studies in statistical mechanics)*. sole distributors for the U.S.A. and Canada, American Elsevier (1976).

[4] A. Einstein. "Zur Theorie der Radiometerkräfte." *Zeitschrift für Physik 27* (1924).

[5] A. Einstein. *The Collected Papers of Albert Einstein, Volume 14 (English): The Berlin Years: Writings & Correspondence, April 1923–May 1925 (English Translation Supplement)-Documentary Edition*. Princeton University Press (2015).

[6] H. Martin. "Reynolds, Maxwell, and the Radiometer, Revisited." In *2010 14th International Heat Transfer Conference*, pp. 111–116. American Society of Mechanical Engineers (2010).

[7] L. Han, S. Wu, J. C. Condit, N. J. Kemp, T. E. Milner, M. D. Feldman, and S. Chen. "Light-Powered Micromotor: Design, Fabrication, and Mathematical Modeling." *Journal of Microelectromechanical Systems*, **volume 20**(2), pp. 487–496 (2011).

[8] J. A. Lockwood. "Neutron measurements in space." *Space Science Reviews*, **volume 14**(5), pp. 663–719 (1973).

[9] G. F. Knoll. *Radiation detection and measurement / Glenn F. Knoll.* Wiley, New York ; Chichester, 2nd ed. edition (1989).

[10] "International Programme of Chemical Safety Notes ICSC: 0231." (2019). URL http://www.inchem.org/documents/icsc/icsc/eics0231.htm.

[11] Y. Gi Kim, P. A. Dowben, J. Spencer, and G. Ramseyer. "Chemical vapor deposition of boron and boron nitride from decaborane (l4) a." (1989).

[12] "Saint Gobain Machineable Ceramics Website." (2019). URL https://www.bn.saint-gobain.com/products/machinable-ceramics.

[13] L. Deng, C. Chen, T. Ye, and G. Li. "The Dosimetry Calculation for Boron Neutron Capture Therapy." In *Diagnostic Techniques and Surgical Management of Brain Tumors*. InTech (2011).

[14] D. J. Bennet and J. R. Thomson. *The Elements of Nuclear Power*. Longman (1989).

[15] L.-H. Han, S. Wu, J. C. Condit, N. J. Kemp, T. E. Milner, M. D. Feldman, and S. Chen. "Light-powered micromotor driven by geometry-assisted, asymmetric photon-heating and subsequent gas convection." *Applied Physics Letters*, **volume 96**(21), p. 213509 (2010).

[16] J. Leppänen, M. Pusa, T. Viitanen, V. Valtavirta, and T. Kaltiaisenaho. "The Serpent Monte Carlo code: Status, development and applications in 2013." *Annals of Nuclear Energy*, **volume 82**, pp. 142–150 (2015).

[17] J. P. Holman. *Heat Transfer*. McGraw-Hill Education (ISE Editions) (1992).